

positive NaX. During ion exchange, Na⁺ detaches from the sediments to replace Ca²⁺ in solution. On the other hand, Ca²⁺ is removed to fill in the void Na⁺ spaces on the rock surface (Li *et al*, 2010). Conversely, the transfer of moles during March 2018 and July 2018 indicated the occurrence of cation exchange instead. This was indicated by a positive value of CaX2 with a negative value of NaX along the same flow path. The occurrence of cation exchange at the same area during these two periods was as a result of high recharge such that sodium ions were flushed out of the system as they were replaced by calcium.

Table 17: Inverse modelling (modelling-approach) results showing mole transfer between two boreholes

Months:	Jul-17	Oct-17	Mar-18	Jul-18
Sampling season	Wet	Dry	Dry	Wet
Water composition	Na-Cl water	Na-Cl water	Na-Cl water	Na-Cl water
TDS (mg/l) between inflow and outflow point	503.1-391.95	19.5-196.3	46.28-23.53	17.446-125.385
Phase mole transfare	BH 9 to BH 8			
Elevation (mamsl)	143-22 m			
Halite	2.19E-02	2.09E-02	8.17E-03	1.85E-02
Gypsum	2.60E-03	4.20E-04	-	-1.99E-05
Kaolinite	5.18E-03	4.53E+01	-	-
Ca-Montmorillon	-4.61E-03	-3.89E+01	-5.79E+01	-1.53E-04
Calcite	6.72E-04	6.41E+00	-5.78E+01	-
Chalcedony	5.38E-03	5.21E+01	-	-5.09E-04
Biotite	4.01E-04	4.33E-04	2.40E-05	3.57E-04
Plagioclase	-	-	9.66E+00	-
Quartz	-	-	-1.78E+02	-
Albite	-	-	1.22E+02	-
CaX2	-2.19E-03	-3.85E-04	6.38E+01	1.45E-03
NaX	4.37E-03	7.70E-04	-1.28E+02	-2.89E-03
Uncertainty (%)	5	5	1.5	1.5

Table 18 indicates the mass-balance modelling results that were generated for flow path from the BH 8 to BH 6. Model simulations were obtained for the periods July 2017, October 2017, March 2018, and July 2018. Uncertainty values of 5% and 1.5% were used to conduct the simulation. The sample for all the sampling periods indicated a Na-Cl water composition as displayed in the Piper diagrams (Figures 16-19). The results indicated by these simulations showed that for July 2017, there was dissolution of halite, kaolinite, biotite, and quartz, though there was also precipitation of Ca-montmorillonite and sylvite. In October 2017, there was precipitation of halite, kaolinite, and biotite however there was dissolution of gypsum and plagioclase. In March 2018, there was dissolution halite, biotite, plagioclase, and albite but there was also precipitation of Ca-montmorillonite, calcite, and quartz. In October 2017, there was dissolution of halite, gypsum, chalcedony, and plagioclase, however there was precipitation of biotite.

The results indicated that ion exchange along this flow path was occurring. The occurrence of ion exchange was indicated by a negative CaX2 value with a positive NaX for October 2017

and July 2018. During ion exchange, Na⁺ detached from the sediments to replace Ca²⁺ in solution. On the other hand, Ca²⁺ was removed to fill in the void Na⁺ spaces on the rock surface (Li *et al.*, 2010). Conversely, the transfer of moles during March 2018 indicated the occurrence of reverse ion exchange instead. This was indicated by a positive value of CaX2 with a negative value of NaX along the same flow path. The occurrence of cation exchange at the same area during these two periods was as a result of high recharge such that sodium ions were flushed out of the system as they were replaced by calcium.

Table 18: Inverse modelling (modelling-approach) results showing mole transfer between two boreholes

Months:	Jul-17	Oct-17	Mar-18	Jul-18
Sampling season	Wet	Dry	Dry	Wet
Water composition	Na-Cl water	Na-Cl water	Na-Cl water	Na-Cl water
TDS (mg/l) between inflow and outflow point	391.95-1826.5	196.3-207.35	23.53-834.6	125.385-407.03
Phase mole transfare	BH 8 to BH 6			
Elevation (mamsl)	23-22 m			
Halite	5.90E-03	-5.63E-03	8.17E-03	2.66E-02
Gypsum	-	3.63E-04	-	1.13E-03
Kaolinite	7.86E-03	-1.81E-04	-	-
Ca-Montmorillon	-6.78E-03	-	-5.79E+01	-
Calcite	-	-	-5.78E+01	-
Chalcedony	-	-	-	5.61E-04
Biotite	7.04E-05	-2.97E-04	2.40E-05	-5.11E-04
Plagioclase	-	4.77E-04	9.66E+00	3.70E-04
Quartz	8.94E-03	-	-1.78E+02	-
Albite	-	-	1.22E+02	-
CaX2	-	-3.14E-04	6.38E+01	-1.43E-03
NaX	-	6.27E-04	-1.28E+02	2.85E-03
Sylvite	-1.00E-04	-	-	-
Uncertainty (%)	5	5	1.5	5

Table 19 indicates the mass-balance modelling results that were generated for flow path from the BH 6 to BH 1. Model simulations were obtained for the periods July 2017, October 2017, March 2018, and July 2018. Uncertainty values of 5% and 1.5% were used to conduct the simulation. The sample for all the sampling periods indicated a Na-Cl water composition as displayed in the Piper diagrams (Figures 16-19). The results indicated by these simulations showed that for July 2017, there was only dissolution of plagioclase, though there was precipitation of kaolinite and biotite. In October 2017, there was precipitation of Ca-montmorillonite, calcite, and chalcedony, however, there was dissolution of halite, gypsum, and biotite. In March 2018, there was dissolution halite, biotite, plagioclase, and albite but there was also precipitation of Ca-montmorillonite, calcite, and quartz. In October 2017, there was dissolution of halite and biotite, however there was precipitation of gypsum, Ca-montmorillonite, and chalcedony.

The results indicated that ion exchange along this flow path was occurring. The occurrence of ion exchange was indicated by a negative CaX2 value with a positive NaX for October 2017. During ion exchange, Na⁺ detached from the sediments to replace Ca²⁺ in solution. On the other hand, Ca²⁺ was removed to fill in the void Na⁺ spaces on the rock surface (Li *et al.*, 2010). Conversely, the transfer of moles during July 2017, March 2018 and July 2018 indicated the occurrence of cation exchange instead. This was indicated by a positive value of CaX2 with a negative value of NaX along the same flow path. The occurrence of cation exchange at the same area during these two periods was as a result of high recharge such that sodium ions were flushed out of the system as they were replaced by calcium.

Table 19: Inverse modelling (modelling-approach) results showing mole transfer between two boreholes

Months:	Jul-17	Oct-17	Mar-18	Jul-18
Sampling season	Wet	Dry	Dry	Wet
Water composition	Na-Cl water	Na-Cl water	Na-Cl water	Na-Cl water
TDS (mg/l) between inflow and outflow point	1826-8034	207.35-664.9	834.6-3952	407.03-1354.73
Phase mole transfare	BH 6 to BH 1			
Elevation (mamsl)	23 - 18 m			
Halite	-	1.18E-02	8.17E-03	1.85E-02
Gypsum	-	2.76E-03	-	-1.99E-05
Kaolinite	-1.23E-04	-	-	-
Ca-Montmorillon	-	-1.77E-04	-5.79E+01	-1.53E-04
Calcite	-	-6.10E-04	-5.78E+01	-
Chalcedony	-	-5.89E-04	-	-5.09E-04
Biotite	-2.03E-04	4.13E-04	2.40E-05	3.57E-04
Plagioclase	3.26E-04	-	9.66E+00	-
Quartz	-	-	-1.78E+02	-
Albite	-	-	1.22E+02	-
CaX2	9.61E-04	-1.74E-03	6.38E+01	1.45E-03
NaX	-1.92E-03	3.48E-03	-1.28E+02	-2.89E-03
Uncertainty (%)	5	5	1.5	1.5

Table 20 indicates the mass-balance modelling results that were generated for flow path from the F5 to BH 4. Model simulations were obtained for the periods July 2017, October 2017, March 2018, and July 2018. Uncertainty values of 2.5%, 5% and 1.5% were used to conduct the simulation. The sample for all the sampling periods indicated a Na-Cl water composition as displayed in the Piper diagrams (Figures 16-19). The results indicated by these simulations showed that for July 2017, there was only dissolution of gypsum and calcite, though there was no precipitation taking place. In October 2017, there was no precipitation taking place, however, there was dissolution of gypsum and calcite. In March 2018, there was dissolution halite and calcite but there was no precipitation taking place. In October 2017, there was dissolution of halite, gypsum, and calcite, however there was no precipitation taking place. The results indicated that ion exchange along this flow path was occurring. The occurrence of ion exchange was indicated by a negative CaX2 value with a positive NaX for July 2017,

October 2017, and July 2018. During ion exchange, Na^+ detached from the sediments to replace Ca^{2+} in solution. On the other hand, Ca^{2+} was removed to fill in the void Na^+ spaces on the rock surface (Li *et al.*, 2010). Conversely, the transfer of moles during March 2018 indicated the occurrence of cation exchange instead. This was indicated by a positive value of CaX2 with a negative value of NaX along the same flow path. The occurrence of cation exchange at the same area during these two periods was as a result of high recharge such that sodium ions were flushed out of the system as they were replaced by calcium.

Table 20: Inverse modelling (modelling-approach) results showing mole transfer between two boreholes

Months:	Jul-17	Oct-17	Mar-18	Jul-18
Sampling season	Wet	Dry	Dry	Wet
Water composition	Na-Cl water	Na-Cl water	Na-Cl water	Na-Cl water
TDS (mg/l) between inflow and outflow point	7319-2450.5	1781-664.5	1943.5-3952	1641.9-1354.73
Phase mole transfare	F5 to BH 4			
Elevation (mamsl)	218-25 m			
Halite	-	-	9.02E-02	1.94E-01
Gypsum	6.65E-03	4.06E-03	-	5.38E-03
Calcite	7.10E-04	9.72E-04	1.27E-03	1.16E-03
CaX2	-2.65E-03	-1.87E-03	2.22E-03	-1.73E-04
NaX	5.31E-03	3.74E-03	-4.44E-03	3.46E-04
Uncertainty (%)	2.5	5	1.5	1.5

4.5 Hydrogeochemical conceptual model development

This section integrates different hydrogeological data to develop a hydrogeochemical conceptual model for the study area. Geology, hydrogeology, recharge/discharge, groundwater flow and hydrology data are used to construct the conceptual model while chemistry data was used to improve and verify the conceptual understanding of the model (Kpegli *et al.*, 2018). The conceptual model provides information on how groundwater flows within the aquifer system. A discussion of how the different hydrogeologic settings influence hydrogeochemical processes in the study area also ensues. Developing an accurate conceptual model is an essential step in the process of a groundwater modelling (Izady *et al.*, 2014).

The lithological logs show that the boreholes (BH 9, BH 11 and BH 13) located upstream are all drilled into the sandstone formation. The boreholes that are drilled in the upper part of the Catchment are drilled in a more mountainous part of the Catchment compared to the lower part of the Catchment. Whereas all the boreholes (BH 4 and BH 6) that are located downstream of the Catchment are drilled primarily into shale and clay except for borehole 3 which is largely drilled into a sand formation. The lithological formation that this drilled into is not surprising given its proximity to the coast and that the area is dominated by sand dunes.

Deep groundwater sampling sites

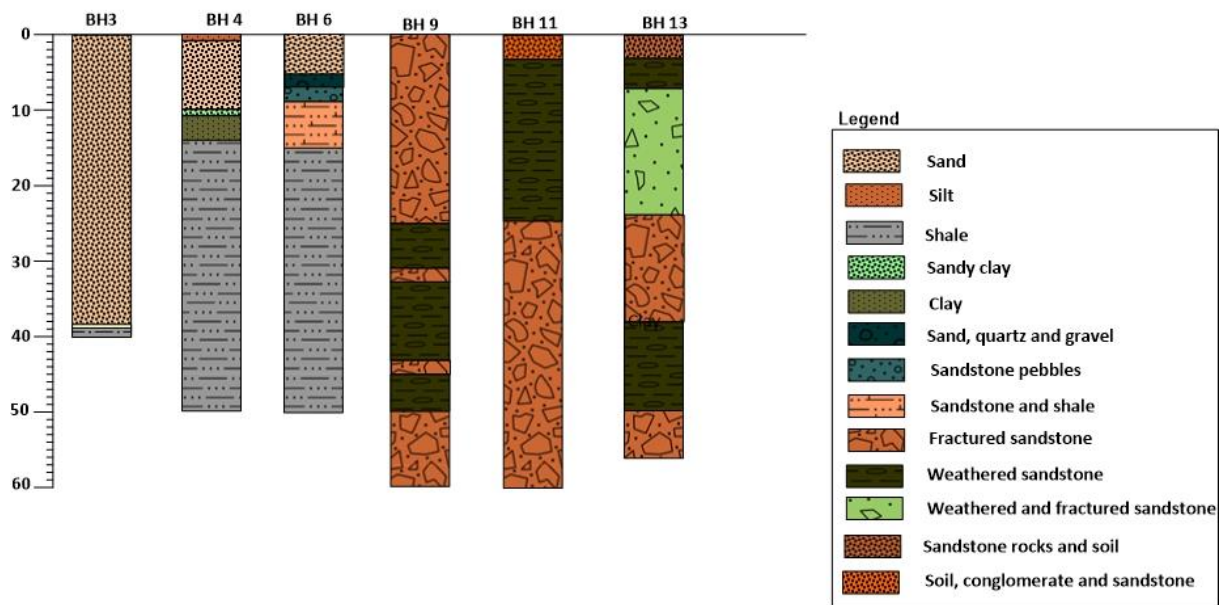


Figure 20: Lithological logs for deep groundwater boreholes in Heuningnes Catchment

The marine clay in the lower part of the study area tends to impede flow (Montcoudiol, 2015), this together with gentle slope of the area can be attributed to the high salinity levels. Flow in the lower parts may be slow as a result of the above-mentioned factors, leading to increased contact time with host geology. The argument by Montcoudiol (2015) supports the results that were found in the current study area, where the low-lying areas with clay in the host geology exhibit high salinity levels compared to those that were recorded in the upper areas of the study area.

The cross-sectional (not drawn to scale) conceptual model (figure 21) for the lower part of the Catchment shows the general flow direction of the groundwater, the lithologies it flows in and the faults in the area.

The groundwater flows from point c to d which is from the middle part of the Catchment towards the coast. The water table in this area is generally close to the surface and during the wet season, this area is usually waterlogged (Mazvimavi, 2018). The boreholes that are in the area mostly drilled into the Bokkeveld series (shale and sandy shale formation). The elevated salinity levels can be attributed to the weathering of the shale formation (Tahoori *et al.*, 2014).

Moddervlei-SANParks (lower Catchment)

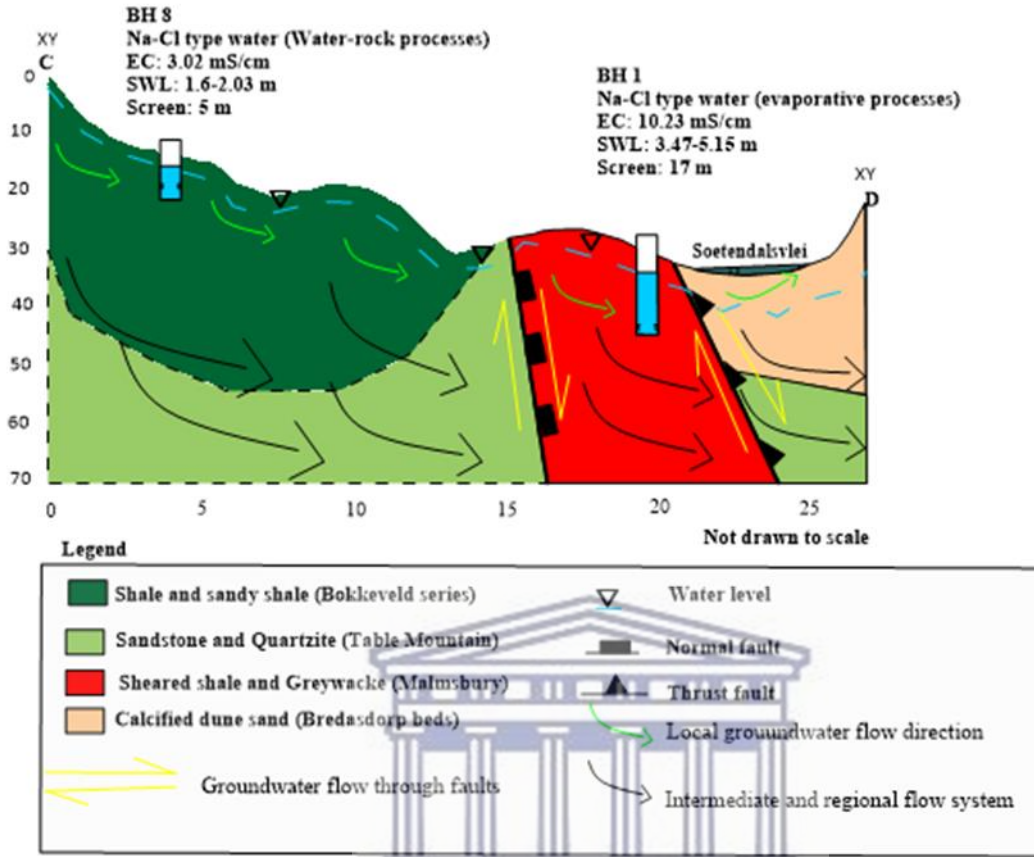


Figure 21: Cross-sectional conceptual model for the Heuningnes Catchment

Figure 22 below shows the major formations in which the aquifer(s) in the study are found in.

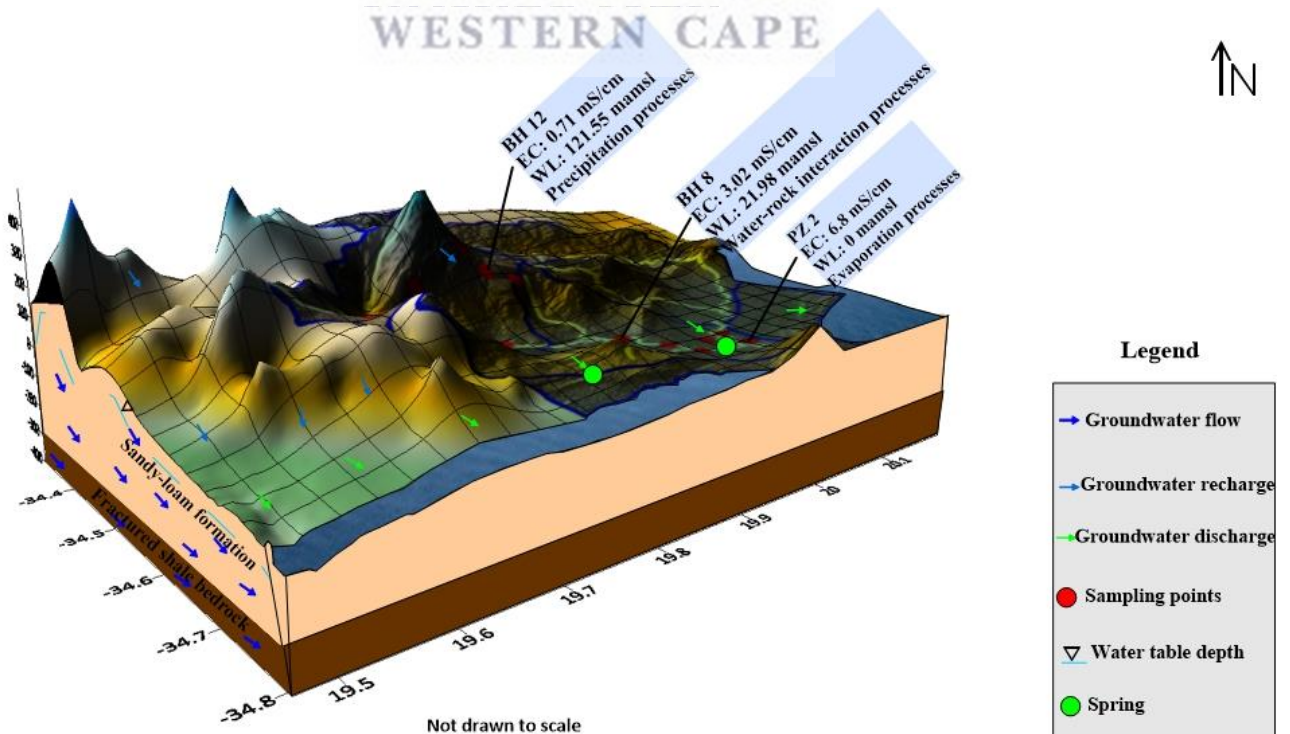
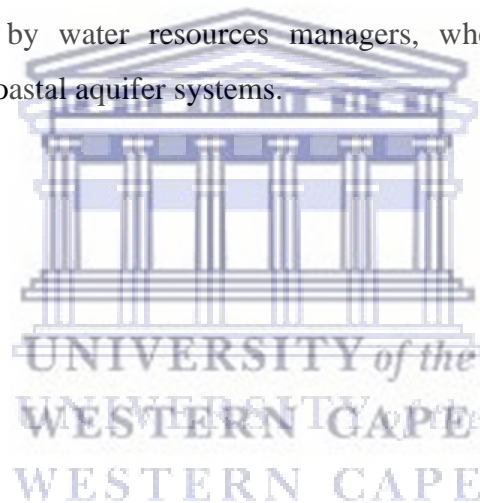


Figure 22: A 3D conceptual model for the Heuningnes Catchment

The boreholes that are drilled in the high altitudes are characterized by low salinity levels but towards the low altitudes in the middle reaches towards the coast salinity begins to rise (0.71 mS/cm, 3.02 mS/cm, and 6.8 mS/cm) as shown in the figure 22. As reported by Mazvimavi (2017), the hydrogeology of the area is influenced by the changes in geology resulting in the main flow not being across the geological boundaries but along the faults. The elevated levels of salinity were expected in the study area and were possibly derived from weathering of the geologic material (rock-water interaction) and/or salinization processes (Tahoora *et al.*, 2014) and given that the shale geology and the calcified dune sands which formed under marine environments (Mazvimavi, 2017).

Implication of hydrogeochemical studies in coastal environments

The results from this study can be used as a base line study for future research in coastal environments. In this way the results will shed light on the likely or possible processes that can be expected in coastal aquifers in turn contributing to the knowledge of these systems. The results can be used by water resources managers, when planning protection and management strategies of coastal aquifer systems.



Chapter 5: Conclusion and Recommendations

5.1 Introduction

This study focused on investigating the hydrogeochemical processes of groundwater within the Heuningnes Catchment by, firstly determining the hydrogeochemical processes using different techniques. The second part was to simulate the hydrogeochemical processes based on the spatiotemporal variation of the parameters using a modelling technique. The last part was to evaluate the existing conceptual models of hydrogeochemical processes through literature review.

5.2 Investigation of the dominant hydrogeochemical process in groundwater

The first objective was to determine hydrogeochemical processes. Water type within the Catchment was characterised as belonging to the Na-Cl water type, during all 4 sampling campaigns. The results generated from the Piper diagrams confirm the dominance of sodium and chloride ions in waters of the Heuningnes Catchment. Despite having different concentrations, the same ions were dominant in the whole Catchment. Groundwater of a Na/Cl type is typical for a Coastal aquifer characterised by saline, deep ancient groundwater. No differences in major ion dominance in groundwater could be established during the duration of the study. Based on the results from Gibbs plots, it was concluded that the dominant processes in July 2017 were evaporation and water-rock interaction, during October 2017, March 2018 and July 2018, the dominant processes were water-rock interaction, evaporation and precipitation, respectively. It was concluded based on bivariate correlation and stoichiometric analysis that cation exchange, adsorption, and evaporation, weathering of carbonates, sulphates and silicate minerals are processes influencing the chemistry of groundwater in the Heuningnes Catchment. Therefore, the first objective of the study focusing on determining hydrogeochemical processes was achieved and the research question was answered with valid reliable data sets.

5.3 Modelling approaches for hydrogeochemical processes and source of groundwater parameters

The process of ion exchange and reverse ion exchange happened at low elevations at the same flow path, although during different periods, and this was related to high recharge in summer. Silicate weathering was experienced at high elevations along the flow path. The major silicate weathering that took place was either releasing montmorillonite or kaolinite. Carbonate and gypsum dissolutions were also experienced at some areas along the flow paths. Meanwhile, dissolution of other minerals such as sylvite and halite were also experienced at random areas along the flow path. The mass-balance modelling results indicated that if more minerals were precipitated from solution, the resulting solution would have a TDS concentration smaller

than that of the initial solution. This was assumed to be happening in areas where Solution 1 was mineralised or had a higher TDS than Solution 2. However, if more minerals were dissolved, the resultant solution becomes more mineralised and its TDS increased. Therefore, the second objective of the study focusing on simulating hydrogeochemical processes was achieved and the research question was answered with valid reliable data sets.

5.4 Assessment of conceptual model for hydrogeochemical processes in groundwater

The third objective was to evaluate the existing conceptual models of hydrogeochemical processes. This was done in order to develop a comprehensive hydrogeochemical conceptual model for the study area. The model was developed based on secondary data from records review and hydrochemical data. The conceptual model for the hydrogeochemical processes in the study area has been supported by the following evidence: The study area has a shallow water table (less than 10 m) both in upstream and downstream areas. The Table Mountain Group (TMG) formation dominant in upstream areas has low salinity values this is as a result of the reduced time of interaction between the water and the host material. Generally, the Bokkeveld series in the study area is characterised by high salinity values due to the layer of shale. Deeper groundwater in the upstream parts of the study area indicates influence of direct recharge without significant evaporation while in the lower areas the dominant process points to evaporation processes. Low surface elevation (gradient) and poor hydraulic conductivity due to the clay layer in the downstream portion of the study area cause slow groundwater flows resulting in high salinization due to the increased residence time. Therefore, the third objective of the study focusing on the evaluation of existing hydrogeochemical conceptual models was achieved and the research question was answered with valid reliable data sets.

Recommendations

The following recommendations were made for future studies:

Sampling should cover a larger area for further studies; thus, more boreholes should be sampled so that there would be no data shortage during the interpretation of results. This will also assist in determining any link on the hydraulic behaviour for different Catchments around the area.

Sample collection may be done for at least four seasons of the year or more in order to make better comparisons of the data; also, to determine any variations in the hydrochemistry of the area.

References

- Abu-alnaeem, M. F., Yusoff, I., Ng, T. F., Alias, Y., and Raksmeiy, M. (2018). Assessment of groundwater salinity and quality in Gaza coastal aquifer, Gaza Strip, Palestine: An integrated statistical, geostatistical and hydrogeochemical approaches study. *Science of the Total Environment*, 615, 972–989. <https://doi.org/10.1016/j.scitotenv.2017.09.320>
- Akpataku, K. V., Rai, S. P., Gnazou, M. D. T., Tampo, L., Bawa, L. M., Djaneye-Boundjou, G., and Faye, S. (2019). Hydrochemical and isotopic characterization of groundwater in the southeastern part of the Plateaux Region, Togo. *Hydrological Sciences Journal*, 64(8), 983–1000. <https://doi.org/10.1080/02626667.2019.1615067>
- Argamasilla, M., Barberá, J. A., and Andreo, B. (2017). Factors controlling groundwater salinization and hydrogeochemical processes in coastal aquifers from southern Spain. *Science of the Total Environment*. <https://doi.org/10.1016/j.scitotenv.2016.11.173>
- Belkhiri, L., Mouni, L., and Tiri, A. (2012). Water-rock interaction and geochemistry of groundwater from the Ain Azel aquifer, Algeria. *Environmental Geochemistry and Health*, 34(1), 1–13. <https://doi.org/10.1007/s10653-011-9376-4>
- Carucci, V., Petitta, M., and Aravena, R. (2012). Interaction between shallow and deep aquifers in the Tivoli Plain (Central Italy) enhanced by groundwater extraction: A multi-isotope approach and geochemical modeling. *Applied Geochemistry*, 27(1), 266–280. <https://doi.org/10.1016/j.apgeochem.2011.11.007>
- Charlier, J. B., Bertrand, C., and Mudry, J. (2012). Conceptual hydrogeological model of flow and transport of dissolved organic carbon in a small Jura karst system. *Journal of Hydrology*, 460–461, 52–64. <https://doi.org/10.1016/j.jhydrol.2012.06.043>
- Chebbah, M., and Allia, Z. (2016). Geochemistry and hydrogeochemical process of groundwater in the Souf valley of Low Septentrional Sahara, Algeria. *African Journal of Environmental Science and Technology*, 9(3), 261–273. <https://doi.org/10.5897/ajest2014.1710>
- Chidambaram, S., Anandhan, P., Prasanna, M. V., Ramanathan, A. L., Srinivasamoorthy, K., and Kumar, G. S. (2012). Hydrogeochemical Modelling for Groundwater in Neyveli Aquifer, Tamil Nadu, India, Using PHREEQC: A Case Study. *Natural Resources Research*, 21(3), 311–324. <https://doi.org/10.1007/s11053-012-9180-6>
- Egbueri, J. C. (2019). Water quality appraisal of selected farm provinces using integrated hydrogeochemical, multivariate statistical, and microbiological technique. *Modeling Earth Systems and Environment*, 0(0), 0. <https://doi.org/10.1007/s40808-019-00585-z>
- El Alfy, M., Lashin, A., Abdalla, F., and Al-Bassam, A. (2017). Assessing the hydrogeochemical processes affecting groundwater pollution in arid areas using an

- integration of geochemical equilibrium and multivariate statistical techniques. *Environmental Pollution*, 229, 760–770. <https://doi.org/10.1016/j.envpol.2017.05.052>
- Elango, L., & Kannan, R. (2007). Rock–water interaction and its control on chemical composition of groundwater, *Developments in environmental science*, 5, 229–243.
- Enemark, T., Peeters, L. J. M., Mallants, D., and Batelaan, O. (2019). Hydrogeological conceptual model building and testing: A review. *Journal of Hydrology*, 569(July 2018), 310–329. <https://doi.org/10.1016/j.jhydrol.2018.12.007>
- Francés, A. P., Lubczynski, M. W., Roy, J., Santos, F. A. M., and Mahmoudzadeh Ardekani, M. R. (2014). Hydrogeophysics and remote sensing for the design of hydrogeological conceptual models in hard rocks - Sardón Catchment (Spain). *Journal of Applied Geophysics*, 110, 63–81. <https://doi.org/10.1016/j.jappgeo.2014.08.015>
- Freeze, R.A., & Cherry, J.A. (1979). *Groundwater*. 2nd Edition, Prentice Hall, Eaglewood Cliff, 604 pp.
- Gibbs, R. J. (1970). Mechanisms controlling world water chemistry. *Science*, 170(3962), 1088–1090.
- Gomo, M., and Vermeulen, D. (2013). Investigation of hydrogeochemical processes in groundwater resources located in the vicinity of a mine process water dam. *Journal of African Earth Sciences*, 86, 119–128. <https://doi.org/10.1016/j.jafrearsci.2013.06.010>
- Hassen, I., Hamzaoui-Azaza, F., and Bouhlila, R. (2018). Establishing complex compartments-aquifers connectivity via geochemical approaches towards hydrogeochemical conceptual model: Kasserine Aquifer System, Central Tunisia. *Journal of Geochemical Exploration*, 188(January), 257–269. <https://doi.org/10.1016/j.gexplo.2018.01.025>
- Hem, J. D. (1985). *Study and interpretation of the chemical characteristics of natural water*. Vol. 2254. Department of the Interior, US Geological Survey.
- Ibrahim, R. G. M., Korany, E. A., Tempel, R. N., and Gomaa, M. A. (2019). Processes of water–rock interactions and their impacts upon the groundwater composition in Assiut area, Egypt: Applications of hydrogeochemical and multivariate analysis. *Journal of African Earth Sciences*, 149(July 2018), 72–83. <https://doi.org/10.1016/j.jafrearsci.2018.07.026>
- Iqbal, J., Nazzal, Y., Howari, F., Xavier, C., and Yousef, A. (2018). Hydrochemical processes determining the groundwater quality for irrigation use in an arid environment: The case of Liwa Aquifer, Abu Dhabi, United Arab Emirates. *Groundwater for Sustainable Development*, 7(April), 212–219. <https://doi.org/10.1016/j.gsd.2018.06.004>
- Izady, A., Davary, K., Alizadeh, A., Ziaei, A.N., Alipoor A, Joodavi, A. and Brusseau, M.L.

- (2014). A framework toward developing a groundwater conceptual model. *Arab J Geosci* 7:3611–3631
- Jamshed, S. (2014). Qualitative research method-interviewing and observation. *Journal of Basic and Clinical Pharmacy*, 5(4), 87. <https://doi.org/10.4103/0976-0105.141942>
- Jia, Z., Zang, H., Hobbs, P., Zheng, X., Xu, Y., and Wang, K. (2017). Application of inverse modeling in a study of the hydrogeochemical evolution of karst groundwater in the Jinci Spring region, northern China. *Environmental Earth Sciences*, 76(8). <https://doi.org/10.1007/s12665-017-6631-8>
- Kalbus E, Reinstorf F and Schirmer M (2006) Measuring methods for groundwater – surface water interactions: a review. *Hydrol. Earth Syst. Sci.*, 10: 873–887
- Kanagaraj, G., Elango, L., Sridhar, S. G. D., and Gowrisankar, G. (2018). Hydrogeochemical processes and influence of seawater intrusion in coastal aquifers south of Chennai, Tamil Nadu, India. *Environmental Science and Pollution Research*, 25(9). <https://doi.org/10.1007/s11356-017-0910-5>
- Kpegli, K. A. R., Alassane, A., van der Zee, S. E. A. T. M., Boukari, M., and Mama, D. (2018). Development of a conceptual groundwater flow model using a combined hydrogeological, hydrochemical and isotopic approach: A case study from southern Benin. *Journal of Hydrology: Regional Studies*, 18(February), 50–67. <https://doi.org/10.1016/j.ejrh.2018.06.002>
- Kumar, M., Kumari, K., Singh, U. K., and Ramanathan, A. (2009). Hydrogeochemical processes in the groundwater environment of Muktsar, Punjab: Conventional graphical and multivariate statistical approach. *Environmental Geology*, 57(4), 873–884. <https://doi.org/10.1007/s00254-008-1367-0>
- Lekula, M., Lubczynski, M. W., and Shemang, E. M. (2018). Hydrogeological conceptual model of large and complex sedimentary aquifer systems – Central Kalahari Basin. *Physics and Chemistry of the Earth*, 106(December 2017), 47–62. <https://doi.org/10.1016/j.pce.2018.05.006>
- Li, Pei-yue, Qian, H., Wu, J., and Ding, J. (2010). Geochemical modeling of groundwater in southern plain area of Pengyang County, Ningxia, China. *Water Sci. Eng.*, 3(3), 282–291. <https://doi.org/10.3882/j.issn.1674-2370.2010.03.004>
- Li, Peiyue, Wu, J., and Qian, H. (2013). Assessment of groundwater quality for irrigation purposes and identification of hydrogeochemical evolution mechanisms in Pengyang County, China. *Environmental Earth Sciences*, 69(7), 2211–2225. <https://doi.org/10.1007/s12665-012-2049-5>
- Li, X., Wu, H., Qian, H., and Gao, Y. (2018). Groundwater chemistry regulated by

- hydrochemical processes and geological structures: A case study in Tongchuan, China. *Water (Switzerland)*, 10(3). <https://doi.org/10.3390/w10030338>
- Lukjan, A., Swasdi, S., and Chalermyanont, T. (2016). Importance of Alternative Conceptual Model for Sustainable Groundwater Management of the Hat Yai Basin, Thailand. *Procedia Engineering*, 154, 308–316. <https://doi.org/10.1016/j.proeng.2016.07.480>
- Luo, W., Gao, X., and Zhang, X. (2018). Geochemical processes controlling the groundwater chemistry and fluoride contamination in the yuncheng basin, China—an area with complex hydrogeochemical conditions. *PLoS ONE*, 13(7), 1–25. <https://doi.org/10.1371/journal.pone.0199082>
- Madlala, T. E. (2015). Determination of groundwater-surface water interaction, upper Berg River catchment. (Msc thesis). University of the Western Cape.
- Manoj, S., Thirumurugan, M., and Elango, L. (2019). Hydrogeochemical modelling to understand the surface water-groundwater interaction around a proposed uranium mining site. *Journal of Earth System Science*, 128(3). <https://doi.org/10.1007/s12040-019-1078-9>
- Marghade, D., Malpe, D. B., and Subba Rao, N. (2019). Applications of geochemical and multivariate statistical approaches for the evaluation of groundwater quality and human health risks in a semi-arid region of eastern Maharashtra, India. *Environmental Geochemistry and Health*, 1. <https://doi.org/10.1007/s10653-019-00478-1>
- Matos, A. P., and Alves, C. (2016). Multivariate statistical analysis of hydrogeochemical data towards understanding groundwater flow systems in granites. *Quarterly Journal of Engineering Geology and Hydrogeology*, 49(2), 132–137. <https://doi.org/10.1144/qjegh2016-006>
- Mazvimavi, D. (2017) Finding “new” water in an “old” catchment: the case of the Heuningnes Catchment, Breede-Overberg Water Management Report. Water Research Commission.
- Montcoudiol, N., Molson, J., Lemieux, J. M., and Cloutier, V. (2015). A conceptual model for groundwater flow and geochemical evolution in the southern Outaouais Region, Québec, Canada. *Applied Geochemistry*, 58, 62–77. <https://doi.org/10.1016/j.apgeochem.2015.03.007>
- Moran-Ramírez, J., Ramos-Leal, J. A., Mahlkecht, J., Santacruz-DeLeón, G., Martín-Romero, F., Fuentes Rivas, R., and Mora, A. (2018). Modeling of groundwater processes in a karstic aquifer of Sierra Madre Oriental, Mexico. *Applied Geochemistry*, 95(February), 97–109. <https://doi.org/10.1016/j.apgeochem.2018.05.011>
- Mouton, J. (2001). How to succeed in your Master’s and Doctoral studies: A South African

guide and resource book. Van Schaik

- Nasher, G., Al-Sayyaghi, A., and Al-Matary, A. (2013). Identification and evaluation of the hydrogeochemical processes of the lower part of Wadi Siham Catchment area, Tihama plain, Yemen. *Arabian Journal of Geosciences*, 6(6), 2131–2146. <https://doi.org/10.1007/s12517-011-0471-8>
- Ntanganedzeni, B., Elumalai, V., and Rajmohan, N. (2018). Coastal aquifer contamination and geochemical processes evaluation in Tugela Catchment, South Africa-Geochemical and statistical approaches. *Water (Switzerland)*, 10(6). <https://doi.org/10.3390/w10060687>
- Parkhurst, D.L. and Appelo, C.A.J. 1999. User's guide to PHREEQC (Version 2) – A computer program for speciation, batch-reaction, one-dimensional transport, and inverse geochemical calculations. U.S. Department of the Interior.
- Pazand, K., Khosravi, D., Ghaderi, M. R., and Rezvanzadeh, M. R. (2018). Identification of the hydrogeochemical processes and assessment of groundwater in a semi-arid region using major ion chemistry: A case study of Ardestan basin in Central Iran. *Groundwater for Sustainable Development*, 6(January), 245–254. <https://doi.org/10.1016/j.gsd.2018.01.008>
- Piper, A. M. (1944). A graphic procedure in the geochemical interpretation of water analyses. *Transactions of the American Geophysical Union* 25, Plenum Press, Boca Raton: 914–928.
- Rajabi, M. M., Ataie-Ashtiani, B., and Simmons, C. T. (2018). Model-data interaction in groundwater studies: Review of methods, applications and future directions. *Journal of Hydrology*, 567(September), 457–477. <https://doi.org/10.1016/j.jhydrol.2018.09.053>
- Rajesh, R., Brindha, K., Murugan, R., and Elango, L. (2012). Influence of hydrogeochemical processes on temporal changes in groundwater quality in a part of Nalgonda district, Andhra Pradesh, India. *Environmental Earth Sciences*, 65(4), 1203–1213. <https://doi.org/10.1007/s12665-011-1368-2>
- Reddy, A. G. S., and Kumar, K. N. (2010). Identification of the hydrogeochemical processes in groundwater using major ion chemistry: A case study of Penna-Chitravathi river basins in Southern India. *Environmental Monitoring and Assessment*, 170(1–4), 365–382. <https://doi.org/10.1007/s10661-009-1239-4>
- Roy, A., Keesari, T., Mohokar, H., Pant, D., Sinha, U. K., and Mendhekar, G. N. (2020). Geochemical evolution of groundwater in hard-rock aquifers of South India using statistical and modelling techniques. *Hydrological Sciences Journal*, 00(00), 1–18. <https://doi.org/10.1080/02626667.2019.1708914>

- Russell, I. A., & Impson, N. D. (2006). Aquatic systems in and adjacent to Agulhas National Park with particular reference to the fish fauna. *Koedoe* 49:45–57. doi:10.4102/koedoe.v49i2.120.
- Senthilkumar, M., and Elango, L. (2013). Geochemical processes controlling the groundwater quality in lower Palar river basin, southern India. *Journal of Earth System Science*, 122(2), 419–432. <https://doi.org/10.1007/s12040-013-0284-0>
- Suma, C. S., Srinivasamoorthy, K., Saravanan, K., Faizalkhan, A., Prakash, R., and Gopinath, S. (2015). Geochemical Modeling of Groundwater in Chinnar River Basin: A Source Identification Perspective. *Aquatic Procedia*, 4(Icwrcoe), 986–992. <https://doi.org/10.1016/j.aqpro.2015.02.124>
- Tahoori S.N, Mohammad F.R, Ahmad Z.A, Wan N.A.S, Hafizan, J, and Kazem, F. (2014). Identification of the hydrogeochemical processes in groundwater using classic integrated geochemical methods and geostatistical techniques, in Amol-Babol Plain, Iran. *The Scientific World Journal*, 2014, 15. <https://doi.org/10.1155/2014/419058>
- Varol, S., and Davraz, A. (2014). Assessment of geochemistry and hydrogeochemical processes in groundwater of the Tefenni plain (Burdur/Turkey). *Environmental Earth Sciences*, 71(11), 4657–4673. <https://doi.org/10.1007/s12665-013-2856-3>
- Vasu, D., Singh, S. K., Tiwary, P., Sahu, N., Ray, S. K., Butte, P., and Duraisami, V. P. (2017). Influence of geochemical processes on hydrochemistry and irrigation suitability of groundwater in part of semi-arid Deccan Plateau, India. *Applied Water Science*, 7(7), 3803–3815. <https://doi.org/10.1007/s13201-017-0528-2>
- Weight, W.D. (2008) *Hydrogeology field manual*. Second edition, McGraw-Hill
- Yang, Q., Li, Z., Ma, H., Wang, L., and Martín, J. D. (2016). Identification of the hydrogeochemical processes and assessment of groundwater quality using classic integrated geochemical methods in the Southeastern part of Ordos basin, China. *Environmental Pollution*, 218, 879–888. <https://doi.org/10.1016/j.envpol.2016.08.017>
- Younger, P.L. 2007. *Groundwater in the environment: An introduction*. Massachusetts: Blackwell Publishing.
- Zhu, C. and Anderson, G. 2002. *Environmental applications of geochemical modelling*. Cambridge: Cambridge University Press.

Appendix 1

Table 21(c): Major Ion concentration of groundwater March 2018 (meq/L)

Site name	Calcium	Sodium	Pottasium	Magnisiurr	Chloride	Sulphate	Bicarbonate
F1	0.25	3.87	0.05	0.99	4.42	0.37	0.30
F2							
F3	0.15	2.30	0.03	0.58	2.79	0.25	0.26
F4							
F5	0.35	2.26	0.03	0.41	2.62	0.06	0.16
BH1	4.14	105.13	0.66	16.45	132.48	19.53	5.21
BH2	25.45	2.00	2.25	41.14	506.60	52.36	6.26
BH3	5.19	1.30	0.51	9.05	112.84	17.40	7.64
BH4	7.29	87.39	0.13	12.34	103.30	11.22	2.69
BH5	5.89	123.26	0.15	13.99	123.30	18.15	2.46
BH6	1.50	22.83	0.05	2.39	22.06	1.12	2.69
BH7	4.49	43.78	0.13	10.70	65.92	7.37	2.23
BH8	0.90	14.91	0.08	1.15	15.84	0.40	5.25
BH9	0.30	1.83	0.03	0.49	2.54	0.21	0.95
BH10	0.65	2.22	0.05	0.58	2.82	0.35	0.98
BH11	0.25	2.52	0.03	0.49	3.10	0.40	0.36
BH12	1.60	5.30	0.08	1.07	5.26	0.69	1.70
BH13	0.20	2.96	0.41	0.82	3.47	0.31	1.21
BH14	0.35	2.91	0.15	0.90	3.15	0.23	1.02
PZ 2	4.34	135.13	0.41	12.34	175.52	7.62	6.00
PZ 7							
PZ 8	11.18	304.78	0.36	32.91	335.00	29.50	2.92
PZ 13							
PZ 14	18.36	366.30	0.69	45.25	481.80	49.03	3.05
PZ 16	4.14	139.57	0.59	18.92	151.96	18.34	5.21
PZ 19							
PZ 26	27.69	501.48	0.36	45.25	622.10	42.16	3.87

Table 21d: Major Ion concentration of groundwater July 2018 (meq/L)

Site name	Calcium	Sodium	Pottasium	Magnesium	Chloride	Sulphate	Bicarbonate
F1	0.20	4.61	0.05	0.90	4.25	0.35	0.30
F2	0.20	3.91	0.05	0.82	3.73	0.29	0.59
F3	0.05	1.61	0.03	0.33	1.68	0.15	0.20
F4							
F5	0.10	2.09	0.05	0.41	2.70	0.02	0.30
BH1	9.98	336.96	1.53	33.73	391.20	19.07	4.43
BH2	34.58	608.70	2.33	41.96	748.10	44.95	5.57
BH3	13.47	244.57	1.38	23.86	260.10	15.74	7.21
BH4	12.67	211.96	0.20	22.21	193.76	10.64	2.59
BH5	12.82	266.30	0.28	28.79	222.60	17.34	2.26
BH6	2.89	347.83	0.10	6.17	46.75	2.41	2.39
BH7	9.03	157.61	0.23	23.04	136.64	9.22	2.07
BH8	3.24	17.04	0.10	2.71	20.80	0.19	5.64
BH9	0.45	1.83	0.05	0.58	2.30	0.23	0.98
BH10	0.50	3.70	0.10	0.99	3.40	0.60	0.46
BH11	0.25	5.30	0.03	1.07	5.62	0.60	0.36
BH12	1.10	6.57	0.08	1.23	3.14	0.67	1.02
BH13	0.20	3.39	0.05	0.82	3.15	0.27	0.26
BH14	0.25	3.35	0.05	0.90	3.30	0.21	0.39
PZ 2	13.32	353.26	1.23	35.38	432.40	10.06	4.66
PZ 7							
PZ 8	22.75	597.83	0.49	43.60	587.60	28.62	1.97
PZ 13							
PZ 14	32.88	706.52	0.61	46.89	928.50	45.82	3.08
PZ 16	11.93	375.00	1.07	37.02	484.50	20.30	4.75
PZ 19							
PZ 26	37.52	690.22	0.13	47.72	714.60	42.91	2.43

Appendix 2

Table 22(a): Stoichiometric analysis results for groundwater, July 2017

Site name	Na/Cl	Ca/HCO ₃	Ca/Ca+SO ₄	Na/Na+Cl	(Ca+Mg)/(HCO ₃ +SO ₄)
F1	0.81	1.31	0.92	0.45	3.31
F2	0.88	0.03	0.96	0.47	43.54
F4	0.88	1.97	0.29	0.47	1.51
F5	0.78	1.31	0.40	0.44	1.32
BH1	1.04	0.89	0.99	0.51	5.22
BH3	0.93	0.42	0.61	0.48	2.60
BH4	0.93	0.17	0.41	0.48	1.45
BH5	0.98	0.88	0.34	0.49	1.72
BH6	1.57	3.31	0.11	0.61	0.34
BH7	1.14	1.22	0.74	0.53	3.56
BH8	1.39	3.46	0.14	0.58	0.44
BH10	0.80	0.43	0.57	0.44	1.80
BH11	1.24	2.35	0.39	0.55	1.10
BH12	1.21	0.74	0.72	0.55	1.46
BH14	0.76	1.71	0.44	0.43	1.45
PZ 7	0.75	0.19	0.40	0.43	1.63
PZ 14	1.01	0.46	0.36	0.50	2.44
PZ 19	0.94	1.26	0.86	0.49	1.21

Table 22b: Stoichiometric analysis results for groundwater, October 2017

Site name	Na/Cl	Ca/HCO ₃	Ca/Ca+SO ₄	Na/Na+Cl	(Ca+Mg)/(HCO ₃ +SO ₄)
F1	0.79	1.27	0.39	0.44	2.09
F2	0.96	1.90	0.36	0.49	2.32
F3	0.83	1.52	0.40	0.45	2.22
F5	0.79	0.46	0.88	0.44	1.61
BH1	0.86	0.51	0.21	0.46	0.75
BH6	0.71	0.55	0.43	0.41	1.36
BH7	0.76	0.75	0.27	0.43	1.33
BH8	0.88	0.18	0.43	0.47	0.74
BH9	0.74	0.83	0.57	0.43	1.48
BH10	0.86	3.55	0.60	0.46	2.07
BH12	0.88	0.65	0.56	0.47	0.93
BH13	0.74	0.61	0.39	0.43	1.47
BH14	0.89	0.91	0.52	0.47	1.58
PZ 2	0.73	1.71	0.47	0.42	2.22

Table 22c: Stoichiometric analysis results for groundwater, March 2018

Site name	Na/Cl	Ca/HCO ₃	Ca/Ca+SO ₄	Na/Na+Cl	(Ca+Mg)/(HCO ₃ +SO ₄)
F1	0.88	0.85	0.40	0.47	1.85
F3	0.83	0.57	0.37	0.45	1.42
F5	0.86	2.13	0.85	0.46	3.36
BH1	0.79	0.79	0.17	0.44	0.83
BH4	0.85	2.71	0.39	0.46	1.41
BH5	1.00	2.39	0.24	0.50	0.96
BH6	1.03	0.56	0.57	0.51	1.02
BH7	0.66	2.01	0.38	0.40	1.58
BH8	0.94	0.17	0.69	0.48	0.36
BH10	0.79	0.66	0.65	0.44	0.92
BH11	0.81	0.69	0.39	0.45	0.98
BH12	1.01	0.94	0.70	0.50	1.11
BH13	0.85	0.16	0.39	0.46	0.67
BH14	0.93	0.34	0.60	0.48	1.01
PZ 2	0.77	0.72	0.36	0.43	1.22
PZ 8	0.91	3.83	0.27	0.48	1.36
PZ 14	0.76	6.02	0.27	0.43	1.22
PZ 16	0.92	0.79	0.18	0.48	0.98
PZ 26	0.81	7.16	0.40	0.45	1.58

Table 22d: Stoichiometric analysis results for groundwater, July 2018

Site name	Na/Cl	Ca/HCO ₃	Ca/Ca+SO ₄	Na/Na+Cl	(Ca+Mg)/(HCO ₃ +SO ₄)
F1	1.08	0.68	0.36	0.52	1.70
F2	1.05	0.34	0.41	0.51	1.16
F3	0.96	0.25	0.26	0.49	1.11
F5	0.77	0.34	0.83	0.44	1.62
BH1	0.86	2.25	0.34	0.46	1.86
BH2	0.81	6.20	0.43	0.45	1.52
BH3	0.94	1.87	0.46	0.48	1.63
BH4	1.09	4.89	0.54	0.52	2.64
BH5	1.20	5.67	0.43	0.54	2.12
BH7	1.15	4.37	0.49	0.54	2.84
BH8	0.82	0.58	0.95	0.45	1.02
BH9	0.80	0.46	0.66	0.44	0.85
BH10	1.09	1.09	0.45	0.52	1.40
BH11	0.94	0.69	0.29	0.49	1.37
BH13	1.08	0.76	0.42	0.52	1.92
BH14	1.02	0.63	0.55	0.50	1.92
PZ 2	0.82	2.86	0.57	0.45	3.31
PZ 8	1.02	11.57	0.44	0.50	2.17
PZ 14	0.76	10.67	0.42	0.43	1.63
PZ 16	0.77	2.51	0.37	0.44	1.95
PZ 26	0.97	15.47	0.47	0.49	1.88